PHYSICAL REVIEW B **80**, 140413(R) (2009)

Room-temperature photomagnetism in the spinel ferrite $(Mn,Zn,Fe)_3O_4$ as seen via soft x-ray magnetic circular dichroism

J. S. Bettinger,[1,*] C. Piamonteze,[2] R. V. Chopdekar,[1] M. Liberati,[3] E. Arenholz,[3] and Y. Suzuki[1,4]
[1]*Department of Materials Science and Engineering, University of California, Berkeley, California 94720, USA*
[2]*Swiss Light Source, Paul Scherrer Institut, CH-5232 Villifier-PSI, Switzerland*
[3]*Advanced Light Source, Lawrence Berkeley National Laboratory, Berkeley, California 94720, USA*
[4]*Materials Science Division, Lawrence Berkeley National Laboratory, Berkeley, California 94720, USA*
(Received 10 August 2009; published 27 October 2009)

We have used x-ray magnetic circular dichroism (XMCD) in conjunction with multiplet simulations to directly probe the origin of photomagnetism in nanocrystalline $(Mn,Zn,Fe)_3O_4$. A photomagnetic effect at room temperature has been observed in these films with HeNe illumination. We have verified an intervalence charge transfer among octahedral Fe cations to account for the increase in magnetization observed at and above room temperature in small magnetic fields. Using XMCD, we demonstrate that the dichroism of Fe in octahedral sites increases by 18% at room temperature, while the dichroism of Fe in tetrahedral sites does not change.

DOI: 10.1103/PhysRevB.80.140413 PACS number(s): 75.30.Gw, 75.50.Tt, 78.20.Ls, 78.70.Dm

Multifunctional materials have received much attention in recent years. They provide model systems in which the interplay among electronic, magnetic, and optical properties can be studied in terms of the charge, orbital, and spin degrees of freedom. Materials which are multifunctional at and above room temperature promise technological advances. A subset of multifunctional materials known as photomagnetic materials have been studied since the discovery of the photomagnetic effect in doped garnets by Teale and Temple in 1967.[1] In photomagnetic materials, an incident optical signal changes the magnetization. Thus far, the photomagnetic effect has been observed in a limited number of material systems. They include the doped garnets,[1] doped spinel ferrites,[2] doped perovskite manganites,[3] ferric borate,[4] amorphous spin glasses,[5] and chalcogenide spinels.[6] In the doped garnets and ferrites, the microscopic origin of the photomagnetism has been largely attributed to light-induced electronic transitions resulting in the redistribution of magnetically anisotropic Fe^{2+} ions.[1,5] While this so-called intervalence charge transfer (IVCT) has been inferred by optical-absorption techniques, there has been no direct experimental evidence that the redistribution gives rise to the enhanced magnetic signal upon incident light.

Recently, photoinduced magnetization (PIM) has been observed in various spinel ferrite systems with short-range magnetic ordering.[5,7] Spinel ferrites have three possible Fe cations on either the tetrahedral (Td) or octahedral (Oh) interstitial sites: Fe^{2+}_{Oh}, Fe^{3+}_{Td}, and Fe^{3+}_{Oh}. Some examples of photomagnetic spinel ferrites include $CoFe_2O_4$ nanoparticles below 170 K,[7] Zn- and Ti-substituted $NiFe_2O_4$ spin glasses below 220 K,[5] and $(Mn,Zn,Fe)_3O_4$ (MZFO) nanocrystalline films at and above room temperature.[8] The PIM has been attributed to a change in anisotropy from a light-induced IVCT. For example, illumination at energies above 1.94 eV was seen to increase the low-field magnetization in nanocrystalline MZFO and has been attributed to an IVCT among octahedral Fe cations: $Fe^{2+}_{Oh}+Fe^{3+}_{Oh}\rightarrow Fe^{3+}_{Oh}+Fe^{2+}_{Oh}$.[8,9] In systems with short-range magnetic ordering, this IVCT redistributes the magnetically anisotropic Fe^{2+}_{Oh} cations leading to an increase in the low-field magnetization.[1,10] However, while the IVCT mechanism has been inferred through optical-absorption methods,[5] it has not been directly confirmed as a root cause for photomagnetism. To prove IVCT as the mechanism for PIM, it is necessary to use a technique that determines the cation magnetization with site and valence specificity as well as any changes in cation magnetization upon illumination.

X-ray absorption spectroscopy (XAS) and x-ray magnetic circular dichroism (XMCD) are used to determine the electronic structure of materials including the site and valence information as well as element-specific magnetization. In spinel ferrites, the Fe XMCD can be decoupled into contributions from the Fe^{2+}_{Oh}, Fe^{3+}_{Td}, and Fe^{3+}_{Oh} cations.[11] Thus XMCD is ideally suited to study the IVCT mechanism. By measuring the dichroism spectra with and without incident light, it is possible to attribute any changes in magnetic properties to a specific cation, including site and valence information.

In this work, we use XAS and XMCD at the Fe $L_{3,2}$ edges in combination with multiplet calculations to examine the origin of room-temperature PIM in MZFO samples. We observe a change in the XMCD effect at the Fe^{2+}_{Oh} and Fe^{3+}_{Oh} edges for nanocrystalline samples at and above room temperature upon HeNe illumination, while no light-induced change in XMCD is observed for either epitaxial films at any temperature or for nanocrystalline samples at lower temperatures. These results provide direct evidence that the IVCT mechanism is the source for the room-temperature PIM in this system.

Two types of $(Mn,Zn,Fe)_3O_4$ thin films were deposited via pulsed laser deposition. Nanocrystalline films of $Mn_{0.5}Zn_{0.6}Fe_{1.9}O_4$ and $Mn_{0.4}Zn_{0.6}Fe_2O_4$ were deposited onto Si substrates at room temperature in a vacuum (10^{-6} torr) background. Epitaxial films of $Mn_{0.5}Zn_{0.5}Fe_2O_4$ were deposited on isostructural spinel $MgAl_2O_4$ substrates at 400 °C in 14 mtorr of a $99\%N_2/1\%O_2$ mixture. XAS and XMCD spectra were measured at beamlines 4.0.2 and 6.3.1 at the Advanced Light Source between 100–300 K. XMCD spectra were obtained in a field of 0.1–0.6 T in total electron yield

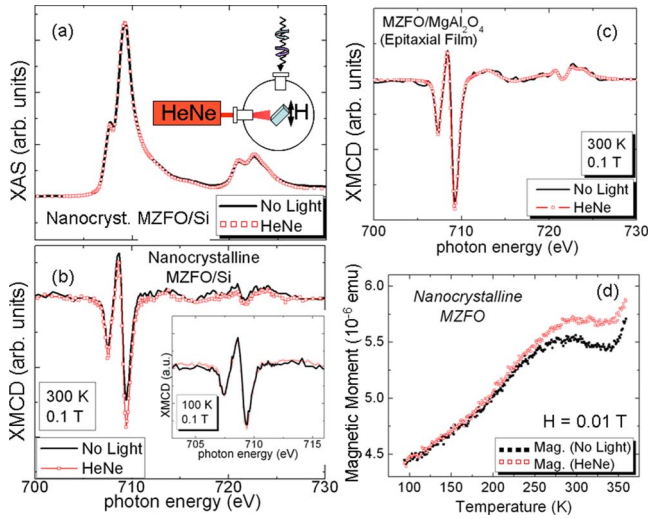

FIG. 1. (Color online) (a) XAS measurements with (red open squares) and without (black solid line) HeNe illumination for a nanocrystalline sample at 300K. Inset: XMCD setup with HeNe. XMCD measurements with (red open squares) and without (black solid line) HeNe illumination for (b) a nanocrystalline sample at 300K (inset: a nanocrystalline sample at 100K) and (c) an epitaxial film at 300K. (d) SQUID measurements with and without HeNe illumination.

mode. The incident photons and applied field (H) were oriented parallel to each other and at a 45° angle from the sample surface. A HeNe laser (1.96 eV) was perpendicular to the photons and field, and also at a 45° angle from the sample [Fig. 1(a) inset], and was used to illuminate samples to determine if there were any change in XMCD. A diffuser ensured that the entire sample was illuminated by the HeNe light. XMCD spectra are obtained by measuring XAS at different fields ($\pm H$). The pre-edges of these XAS measurements are normalized and subtracted from each other to get a difference which is then divided by the difference in absorption between the peak XAS and the pre-edge.

XAS and XMCD spectra were simulated using ligand field multiplet (LFM) theory.[12,13] In LFM calculations, the atomic spectra is calculated by Cowan's[14] Hartree-Fock code where the *d-d* and *p-d* Slater integrals and spin-orbit coupling parameters are calculated. The crystal-field splitting is included after using a group theory approach developed by Butler.[15] The parameters used for the simulation were the same as in previous simulations for Fe_3O_4.[11] The *d-d* and *p-d* Slater integrals were reduced by 70% and 80%, respectively, to account for screening and hybridization. The relative average energy values for Fe^{2+}_{Oh}, Fe^{3+}_{Td}, and Fe^{3+}_{Oh} were obtained from an experimental spectrum of Fe_3O_4, where the proportion of each Fe site is known. These energy shifts were then used in the fits presented for the MZFO data.

In Fig. 1(a), the room-temperature XAS is measured with and without light for a nanocrystalline sample. This line shape does not change markedly with illumination. The room-temperature XMCD is measured with and without light in a field of 0.1 T for both a nanocrystalline [Fig. 1(b)] and epitaxial [Fig. 1(c)] sample. In each measurement, three main features are observed at the Fe L_3 edge which are generally associated with Fe^{2+}_{Oh}, Fe^{3+}_{Td}, and Fe^{3+}_{Oh}, in order of increasing energy.[11] At room temperature, HeNe light has a significant effect on the dichroism of the nanocrystalline sample under the application of a field of 0.1 T. This result will be discussed in greater detail in Fig. 4. At 100 K [Fig. 1(b) inset], there is no change in the line shape. In epitaxial MZFO, there is no change in the XMCD line shape with incident light at any temperature. Moreover, at higher fields (0.5 T) the incident light does not give rise to changes in the dichroism for nanocrystalline and epitaxial samples.

These results are consistent with superconducting quantum interference device (SQUID) magnetometry measurements where PIM was only observed at and above room temperature in nanocrystalline MZFO [Fig. 1(d)]. Here, the zero-field cooled magnetization for a nanocrystalline sample was measured in a field of 0.01 T with and without illumination. There is no PIM at low temperatures, but near room temperature there is a significant increase in magnetic moment upon illumination. The magnetic properties of nanocrystalline MZFO are dominated by its magnetocrystalline anisotropy (MCA). At low temperatures, the MCA is negative but goes through a zero crossing near room temperature, which is well below the Curie temperature. The small magnetic anisotropy has a large effect on the magnetic properties of the system, including the permeability, which undergoes a local maximum at the temperature of the MCA zero crossing.[16] This phenomenon explains the observation of a change in XMCD upon illumination with an applied field of 0.1 T in nanocrystalline MZFO at room temperature and not at 100 K. SQUID magnetometry studies revealed no photomagnetism at fields above 0.2 T.[8] When the field is high enough to initially align the Fe^{2+}_{Oh} cations, then the light will not have any additional effect, and thus we do not observe any light-induced change in XMCD at 0.5 T. No change was observed with illumination in the XAS at any field indicating that there is no net change in Fe cation site occupancy in the system. In both XMCD and SQUID based studies, the photomagnetic effect was found to be irreversible.

SQUID-magnetometry based studies revealed no photomagnetism on epitaxial films at any temperature.[8] When nanocrystalline samples have a zero crossing in the MCA, there is very little anisotropy in the system, and thus it is relatively easy to alter the magnetic properties with light. Epitaxial films, on the other hand, have magnetic properties dominated by shape and magnetoelastic effects and therefore do not have a region of very low total anisotropy well below the Curie temperature that the nanocrystalline samples have. Additionally, a short range in magnetic ordering is necessary for a spinel ferrite to exhibit the photomagnetic effect due to an IVCT. In a material with long-range order, such as an epitaxial film, there is strong exchange coupling throughout, and a valence transfer would have a small effect on the magnetic moment, whereas in the case of nanocrystallites with short-range order, the effect is much larger. We have also shown that smaller nanocrystallite size corresponds to a larger photomagnetic effect.[8]

The low-field magnetization increased with increasing temperature for nanocrystalline MZFO [Fig. 1(d)] as the MCA moves close to zero. For epitaxial films, which have long-range order and magnetic properties dominated by

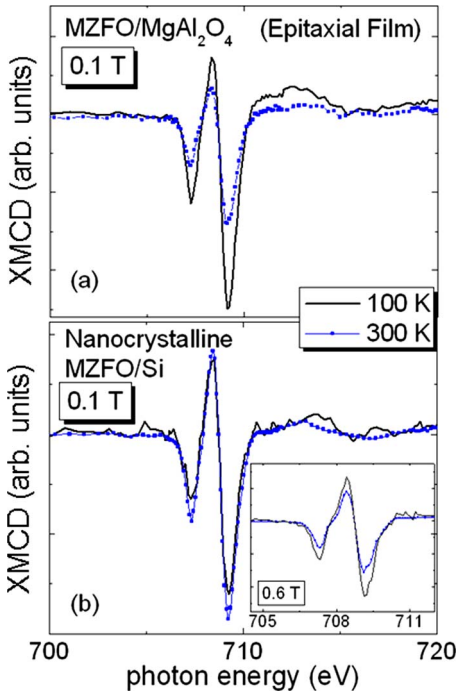

FIG. 2. (Color online) Fe XMCD scans taken at 0.1 T at 100 K (black lines) and 300 K (blue dotted lines) for (a) epitaxial MZFO and (b) nanocrystalline MZFO. Inset: Fe XMCD at 0.6 T for nanocrystalline MZFO.

shape and magnetoelastic effects, the magnetization decreased monotonically with increasing temperature.[8] We have probed this temperature dependence using XMCD in a field of 0.1 T. In Fig. 2(a), the Fe L_3 XMCD for an epitaxial film is shown at 100 and 300 K. The dichroism decreases with increasing temperature at all three features, which can roughly be attributed to Fe^{2+}_{Oh}, Fe^{3+}_{Td}, and Fe^{3+}_{Oh}.[11] In nanocrystalline MZFO [Fig. 2(b)], however, there is actually a small increase in dichroism when the temperature is increased from 100 to 300 K due to an increase in permeability when the MCA is very low. When the nanocrystalline sample is saturated and the properties are no longer dominated by the initial permeability, the dichroism decreases with increasing temperature [Fig. 2(b) inset].

Multiplet simulations were performed to understand the effect of illumination on the XAS and XMCD spectra. Figures 3(a) and 3(b) show the XAS and XMCD simulations, respectively, for the three different Fe cations found in MZFO: Fe^{2+}_{Oh}, Fe^{3+}_{Td}, and Fe^{3+}_{Oh}. In the XAS, the energy position of the absorption edge is greater for higher Fe valence and for the Oh site relative to the Td site. The sign of the dichroism signal is opposite for the Td cation compared to the Oh cation because the spins of magnetic cations on the Td and Oh sites in a spinel are aligned antiparallel to one another.

To quantify the effect of light on the magnetic properties of nanocrystalline MZFO, we have used a weighted average of the calculated spectra to fit the Fe-XMCD measurements with and without illumination (Fig. 4) in applied magnetic fields that are too low to saturate the sample because PIM is not observed once the sample is saturated. We are using mul-

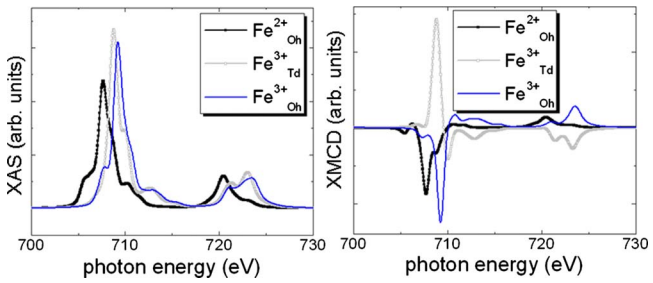

FIG. 3. (Color online) Multiplet simulations of the (a) XAS and (b) XMCD for the Fe^{2+}_{Oh} (closed black squares), Fe^{3+}_{Td} (open gray circles), and Fe^{3+}_{Oh} (solid blue lines) cations in spinel MZFO.

tiplet simulations to quantify the relative change in dichroism that occurs with illumination. The magnitude of the dichroism signal can be thought of as a snapshot of how efficiently the magnetization is aligned by an external field at a given temperature. The simulations indicate that there is a significant change in dichroism upon illumination associated with the Fe^{2+}_{Oh} and Fe^{3+}_{Oh} cations: an increase of approximately 18% with light was seen at both of the Oh edges. While there appears to also be a shift in the Td peak, this is actually due to secondary effects from the Oh cations, and the quantified dichroism associated with the Fe^{3+}_{Td} cation does not change with light.

Using XMCD, we have determined the mechanism for room-temperature PIM observed in MZFO. There are three possible IVCTs in this system: (i) between Fe and Mn cations, (ii) between Mn cations only, or (iii) between Fe cations only. Each of these cases will be discussed individually. (i) The MZFO system contains both Mn and Fe with multiple valences and site symmetries. If an IVCT were to occur among Fe and Mn cations (either $Fe^{2+}_{Oh}+Mn^{3+}_{Oh}\rightarrow Fe^{3+}_{Oh}+Mn^{2+}_{Oh}$ or $Fe^{3+}_{Oh}+Mn^{2+}_{Oh}\rightarrow Fe^{2+}_{Oh}+Mn^{3+}_{Oh}$) then there should be a change in the saturated value of the dichroism; however, no change in XMCD was observed upon illumination at 0.5 T. Additionally, if there were an IVCT occurring between Fe and Mn cations, there would be a net change in the XAS line

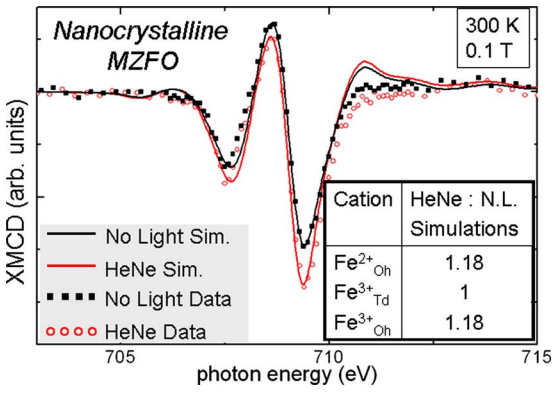

FIG. 4. (Color online) Comparison of experimental XMCD (red open circles with HeNe and black closed squares without HeNe) to multiplet simulations (red or dark gray line with HeNe and black line without HeNe) for photomagnetic MZFO at 300 K. There is an 18% increase in Fe^{2+}_{Oh} and Fe^{3+}_{Oh} XMCD but no change in Fe^{3+}_{Td} XMCD upon illumination.

shape but no such change was seen, indicating that there is no IVCT occurring between Fe and Mn cations. (ii) It is also possible that there is an IVCT occurring between Mn cations only: $Mn^{2+}_{Oh}+Mn^{3+}_{Oh}\rightarrow Mn^{3+}_{Oh}+Mn^{2+}_{Oh}$. We were not able to observe this effect within the current sensitivity of the experiment. Therefore we conclude that this is not the primary mechanism for the photomagnetism in MZFO. (iii) We observed a significant increase in dichroism associated with the Fe^{2+}_{Oh} and Fe^{3+}_{Oh} cations at 0.1 T but no change in the Fe^{3+}_{Td} cations. This increased low magnetic field dichroism associated with the Oh cations without any accompanying change in the Td cations indicates that the Fe^{2+}/Fe^{3+} IVCT mechanism at the Oh sites is responsible for the photomagnetism in these samples.

While XMCD measurements showed an 18% increase in the Oh Fe dichroism with light at 0.1 T, corresponding SQUID measurements showed only a 3% increase with light at the same field.[8] This discrepancy may be attributed to the fact that SQUID magnetometry measures the magnetization of the entire film whereas XMCD is a surface sensitive technique that probes approximately 5–10 nm below the surface. Optical absorption measurements indicate that the epitaxial film has an absorption length of approximately 160 nm at 1.96 eV which provides an upper bound for the more disordered nanocrystalline samples. Since the nanocrystalline film thickness is approximately 300 nm, it is likely that the effect of the incident light does not extend throughout the films so that the more surface sensitive XMCD technique gives rise to a larger PIM when compared to the photomagnetic signal from SQUID measurements. In addition, since the total magnetic signal is derived from the sum of the contributions from the Fe and Mn ions, it is not surprising that the PIM from the Oh Fe dichroism is larger than that from the SQUID measurements that measures the contributions from all magnetic ions.

In conclusion, we used multiplet simulations and XMCD with and without HeNe illumination to verify the proposed mechanism of photomagnetism in MZFO, which is an IVCT between Oh Fe cations. The low-field dichroism of the Fe^{2+}_{Oh} and Fe^{3+}_{Oh} cations significantly increased with illumination from a HeNe laser thereby proving Fe-Fe IVCT as the mechanism for PIM. Future studies to determine the contribution of the orbital moment in the nanocrystalline and epitaxial samples may shed further light on the differences in magnetic anisotropy and hence PIM observed in these samples.

The authors would like to thank A. Cruz. This work has been funded by the Office of Naval Research Grant No. N00014-06-1-0452. The Advanced Light Source is supported by the Director, Office of Science, Office of Basic Energy Sciences, of the U.S. Department of Energy under Contract No. DE-AC02-05CH11231.

*joannabettinger@berkeley.edu

[1] R. W. Teale and D. W. Temple, Phys. Rev. Lett. **19**, 904 (1967).
[2] K. Hisatake, Y. Nagata, and K. Ohta, Jpn. J. Appl. Phys. **15**, 1823 (1976).
[3] M. Baran, S. L. Gnatchenko, O. Y. Gorbenko, A. R. Kaul, R. Szymczak, and H. Szymczak, Phys. Rev. B **60**, 9244 (1999).
[4] D. E. Lacklison, J. Chadwick, and J. L. Page, J. Appl. Phys. **42**, 1445 (1971).
[5] M. Seki, A. K. M. A. Hossain, H. Tabata, and T. Kawai, Solid State Commun. **133**, 791 (2005).
[6] W. Lems, P. J. Rijniers, P. F. Bongers, and U. Enz, Phys. Rev. Lett. **21**, 1643 (1968).
[7] A. K. Giri, E. M. Kirkpatrick, P. Moongkhamklang, S. A. Majetich, and V. G. Harris, Appl. Phys. Lett. **80**, 2341 (2002).
[8] J. S. Bettinger, R. V. Chopdekar, and Y. Suzuki, Appl. Phys. Lett. **94**, 072505 (2009).
[9] W. F. J. Fontijn, P. J. van der Zaag, L. F. Feiner, R. Metselaar, and M. A. C. Devillers, J. Appl. Phys. **85**, 5100 (1999).
[10] J. Kanamori, Prog. Theor. Phys. **17**, 177 (1957).
[11] R. A. D. Pattrick, G. Van der Laan, C. M. B. Henderson, P. Kuiper, E. Dudzik, and D. J. Vaughan, Eur. J. Mineral. **14**, 1095 (2002).
[12] F. M. F. de Groot, J. Electron Spectrosc. Relat. Phenom. **67**, 529 (1994).
[13] G. van der Laan and B. T. Thole, Phys. Rev. B **43**, 13401 (1991).
[14] R. D. Cowan, *The Theory of Atomic Structure and Spectra* (University of California Press, Berkeley, 1982).
[15] P. H. Butler, *Point Group Symmetry Applications: Methods and Tables* (Plenum Press, New York, 1981).
[16] K. Ohta, J. Phys. Soc. Jpn. **18**, 685 (1963).